World Academy of Science, Engineering and Technology
International Journal of Mechanical and Mechatronics Engineering
Vol:4, No:11, 2010

A Study of Various Numerical Turbulence Modeling Methods in Boundary Layer Excitation of a Square Ribbed Channel

Hojjat Saberinejad, Adel Hashiehbaf, Ehsan Afrasiabian

***Abstract*—**Among the various cooling processes in industrial applications such as: electronic devices, heat exchangers, gas turbines, etc. Gas turbine blades cooling is the most challenging one. One of the most common practices is using ribbed wall because of the boundary layer excitation and therefore making the ultimate cooling. Vortex formation between rib and channel wall will result in a complicated behavior of flow regime. At the other hand, selecting the most efficient method for capturing the best results comparing to experimental works would be a fascinating issue. In this paper 4 common methods in turbulence modeling: standard k-e, rationalized k-e with enhanced wall boundary layer treatment, k-w and RSM (Reynolds stress model) are employed to a square ribbed channel to investigate the separation and thermal behavior of the flow in the channel. Finally all results from different methods which are used in this paper will be compared with experimental data available in literature to ensure the numerical method accuracy.

***Keywords*—**boundary layer, turbulence, numerical method, rib cooling

I. INTRODUCTION

VARIOUS cooling methods in gas turbine industries are widely used and related researches are in demand. Different ribbed internal cooling ducts with difference in shape and configuration are studied in recently researches. Whereas it has a turbulent nature with some complicated phenomena such as separation and secondary flows, it is very important to predict behavior of the flows considering the cooling capability.

It seems that Computational Fluid Dynamics (CFD) is the best way to simulate and predict such flows. Considering that high computational expense for simulating such flows is a major obstacle, it would be advantageous to reduce costs. It is possible with engaging economic methods with low computational costs. It is useful to show which method is powerful with low expense such as $k-\varepsilon, k-\omega, RSM$ in comparison with expensive methods such as Large Eddy Simulation (LES) or Direct Numerical Simulation (DNS). Regarding to this fact that LES and DNS consider more details of the flow, but they are cumbersome and need powerful facilities and are applicable only for low Reynolds flows. These issues have limited use of these turbulence methods in the industries and have reduced it to the confined research area. For the purpose of applying turbulence methods in cooling, it is important consider which one is more capable to predict thermal effects.

Some heat transfer experiments have been done in both developing flow by Han and Park [1], Liou and Hwang [2], Wagner et al. [3], Wang et al. [4], Chang and Morris [6], fully developed flow by Han [7], Liou and Hwang [8], Baughn and Yan [9], Fann et al. [10], Park et al. [11], Mochizuki et al. [12], Ekkad et al. [13], Chen et al. [14], Islam et al. [15], Rau et al. [16]. Also some experimental efforts have been done with Laser Doppler Velocimeter (LDV) such as Rau et al. [16], Sato et al. [17], Liou et al. [18], and Graham et al. [19] and hot-wire anemometer measurements by Hirota et al. [20].

Studies using the economic turbulence models have been presented such as $k-\varepsilon$ model by Durst et al. [21], Liou et al. [22], Acharya et al. [23], Prakash and Zerkle [24], Zhao and Tao [25], Ooi et al. [26], $v2-f$ model by Ooi et al. [26] and LES model (Experimental validation of large eddy simulations of flow and heat transfer in a stationary ribbed duct) Sewall et al. [27], Saha and Acharya [28], Tafti [29], Abdel-Wahab and Tafti [30]. Other studies to comparing various methods by Bonhoff et al. [31], Lin et al. [32], Jang et al. [33], Al-Qahtani et al. [34-35], Murata and Mochizuki [36].

In our work both developing and fully developed flows have been considered in a stationary squared duct with two smooth walls and two ribbed walls with an inline configuration. Rib height to hydraulic diameter $(e/D_h)=0.1$ and the rib pitch to height are $(P/e)=10$ and Reynolds on bulk velocity and hydraulic diameter is 20000. There are 9 squared ribs, Walls temperature has been set to $1200^0 k$ and entrance flow is uniform.

Results show that some methods are more suitable and more efficient in thermal modeling in comparison with other ones. In this Paper results are validated with experiments at Re=10000 and 20000 captured with LDV and LES modeling in a stationary ribbed duct. It shows good analogy and leads us to choose an optimum method for internal cooling phenomena with less costs and applicable results. Results show that $k-\varepsilon$ realizable with enhanced wall treatment (two layer approach)

Hojjat Saberinejad Islamic Azad University of langaroud branch, Iran (corresponding author to provide phone; fax: +98-142-524-4422; e-mail: h_saberinejad@iaul.ac.ir).

Adel Hashiehbaf, Abbaspur University of Technology. Abbaspur Blvd,Tehranpars,Tehran,Iran+982144241405,email:adelhashiehbaf@stud.pwut.ac.ir

Ehsan Afrasiabian, Abbaspur University of Technology. Abbaspur Blvd,Tehranpars,Tehran,Iran+982122283696,email:e_afrasiabian@stud.pwut.ac.ir

and fine meshes near the walls have a great capability and acceptable tolerances in according the low computational expenses and could be engaged for higher Reynolds number flows which LES or DNS are not practical.

II. THEORITICAL METHOD

The turbulent flow and heat transfer simulation of the three dimensional channel with square ribs were presented by the steady and unsteady-state Navier-stokes and energy equations. Among the four methods for capturing the flow and temperature field inside the channel, the $k-\varepsilon$ methods and $k-\omega$ methods were solved in steady mode and Reynolds stress model (RSM) in unsteady mode. The average Reynolds governing equation that describe the turbulent flow and energy were defined as follow

$$\begin{cases} \rho\dfrac{\partial k}{\partial t}+\rho u_j k_{,j}=(\mu+\dfrac{\mu_t}{\sigma_k}k_{,j})+G_k+G_b-\rho\varepsilon \\ \rho\dfrac{\partial \varepsilon}{\partial t}+\rho u_j \varepsilon_{,j}=(\mu+\dfrac{\mu_t}{\sigma\varepsilon}\varepsilon_{,j})+C_1\dfrac{\varepsilon}{k}G_k+C_1(1-C_3)\dfrac{\varepsilon}{k}G_b-C_2\rho\dfrac{\varepsilon^2}{k} \end{cases} \quad (1)$$

In which the C_1, C_2, C_3 are experimental constants and σ_k *and* σ_ε are also turbulent prandtl numbers for k and ε, respectively. The terms $C_1(\frac{\varepsilon}{k})G$ *and* $C_2\rho(\frac{\varepsilon^2}{k})$ are representatives of shear generation and viscose dissipation processes, respectively. The term $C_1(1-C_3)(\frac{\varepsilon}{k})B$ is also representative of buoyancy effects. The generation of turbulent kinetic energy due to mean velocity gradients, (G_k) is defined as follow:

$$G_k=-\rho\overline{u_i'u_j'}u_{i,j}\approx\mu_t(u_{i,j}+u_{j,i})u_{i,j} \quad (2)$$

The generation of turbulent kinetic energy due to buoyancy, (G_b) for constant density will be obtained as follow:

$$G_b=g_i[\frac{\mu_t}{\sigma_t}B_T T_{,i}+\frac{\mu_t}{S_t}\beta_c C_{,i}] \quad (3)$$

In addition, the constants are prescribed in Tab.1

TABLE I VALUE FOR CONSTANTS IN $k-\varepsilon$ MODEL

Coefficient	σ_k	σ_ε	C_1	C_2	C_μ
Value	1	1.3	1.44	1.92	0.09

A .k-ε *realizable Model*

As a matter of fact, the standard $k-\varepsilon$ model is not so strong in the separation and swirling flows. It was seen that the $k-\varepsilon$ model tends to predict the over diffusive profiles for swirling flows and shorter recirculation area for separation flows. It means that the turbulent viscosity which is predicted with this model is greater than the real situation. Due to these defects, some advanced $k-\varepsilon$ models were considered to investigate the flow field around a square duct (separation flow) in this paper.

The first model was realizable $k-\varepsilon$ model with enhanced wall treatment instead of using wall functions. This model has two great advantages in comparison with standard wall function:

The model contains a new formulation for turbulent viscosity.

A new transport equation for the dissipation rate, ε, has been derived from an exact equation for the transport of the mean-square vorticity fluctuation.

The model used in this paper, is developed by Shih [5]. He considered the variable C_μ and modified the coefficients of standard $k-\varepsilon$ model. The transport equation for k and ε are as follow:

$$\begin{cases} \dfrac{\partial}{\partial t}(\rho k)+\dfrac{\partial}{\partial x_j}(\rho k u_j)=\dfrac{\partial}{\partial x_j}[(\mu+\dfrac{\mu_t}{\sigma_k})\dfrac{\partial k}{\partial x_j}]+G_k+G_b-\rho\varepsilon+S_k \\ \dfrac{\partial}{\partial t}(\rho\varepsilon)+\dfrac{\partial}{\partial x_j}(\rho\varepsilon u_j)=\dfrac{\partial}{\partial x_j}[(\mu+\dfrac{\mu_t}{\sigma_\varepsilon})\dfrac{\partial k}{\partial x_j}]+\rho C_1 S_\varepsilon-\rho C_2\dfrac{\varepsilon^2}{k+\sqrt{\nu\varepsilon}}+\ldots \\ \ldots+C_{1\varepsilon}\dfrac{\varepsilon}{k}C_{3\varepsilon}G_b+S_k \end{cases} \quad (4)$$

The terms, S_k and S_ε are source terms. The C_1 will be defined as below:

$$C1=\max[0.43,\frac{\eta}{\eta+5}] \qquad \eta=S\frac{k}{\varepsilon} \qquad S=\sqrt{2S_{ij}S_{ij}} \quad (5)$$

According to Eq. (4), the transport equation for k is the same as the in the standard $k-\varepsilon$ model except for the model constants. Two important features of Eq. (4) are as below:

The first term doesn't involve the G_k term (like standard $k-\varepsilon$ model) and this property predicts the energy transfer much better than the standard model.

The second term in the right hand side of transport equation in Eq. (4) never vanishes although the K vanishes and thus doesn't have singularity.

The model for predicting the turbulent viscosity is also modeled as follow:

$$\begin{aligned} \mu_t &= \rho C_\mu \frac{k^2}{\varepsilon} \\ C_\mu &= \frac{1}{A0+A_S\dfrac{kU^*}{\varepsilon}} \\ U^* &\equiv \sqrt{S_{ij}S_{ij}+\tilde{\Omega}_{ij}\tilde{\Omega}_{ij}} \\ \tilde{\Omega}_{ij} &= \Omega_{ij}-2\varepsilon_{ijk}\omega_k \\ \Omega_{ij} &= \overline{\Omega_{ij}}-\varepsilon_{ijk}\omega_k \end{aligned} \quad (6)$$

Where $\overline{\Omega_{ij}}$ is the mean rate-of-rotation tensor viewed in a rotating reference frame with the angular velocity $\overline{\omega_k}$. The constants are represented in Eq. (7).

$$A_0 = 4.04 \qquad A_s = \sqrt{6}\cos\phi$$
$$\phi = \frac{1}{3}\cos^{-1}(\sqrt{6}W) \qquad W = \frac{S_{ij}S_{jk}S_{ki}}{\tilde{S}^3} \tag{7}$$
$$\tilde{S} = \sqrt{S_{ij}S_{ij}} \qquad S_{ij} = \frac{1}{2}(\frac{\partial u_j}{\partial x_j} + \frac{\partial u_i}{\partial x_i})$$

B. k-ω Model

The next method used in this paper is Wilcox $k-\omega$ model. From the comparison aspect, this model is stronger than the standard $k-\varepsilon$ model in flows containing the deceleration and also separation flow due to adverse pressure gradient. It should be noticed that this model is powerful when the Re number is low. The constitutive Equations are as below:

$$\begin{cases} \rho\dfrac{\partial k}{\partial t} + \rho u_j k_{,j} = (\mu + \dfrac{\mu_t}{\sigma_k}k_{,j}) + G_k + G_b - \rho\omega k \\ \rho\dfrac{\partial \varepsilon}{\partial t} + \rho u_j \omega_{,j} = (\mu + \dfrac{\mu_t}{\sigma_\varepsilon}\omega_{,j}) \\ + C_1\dfrac{\omega}{k}G_k + C_1(1-C_3)\dfrac{\omega}{k}G_b - C_2\,\rho\omega^2 \end{cases} \tag{8}$$

The constants are also illustrated in Tab.2.

TABLE II VALUE FOR CONSTANTS IN $k-\omega$ MODEL

Coefficient	σ_k	σ_ε	C_μ	C_1	C_2
Value	2	2	0.09	0.555	0.8333

As it is clear in Eq. (8), the general form of transport equations are so similar to Eq. (1). And instead of using ε, the ω is replaced. So it is clear that the results will be nearly the same for the $k-\varepsilon$ model and $k-\omega$ model.

C. Reynolds Stress Model

The eddy Viscosity models in the attached boundary layer flow are valid when just one element of Reynolds stress tensor is dominant (u'^2). Therefore, the next model was dedicated to RSM model but with the same wall function for near wall regions as for standard $k-\varepsilon$. This was done because of comparison with standard $k-\varepsilon$ model and the importance of other elements of stress tensor for the case study involved in this paper.

The transport equation for turbulence kinetic energy is written as below:

$$\frac{\partial}{\partial t}(\rho k) + \frac{\partial}{\partial x_i}(\rho k u_i) = \frac{\partial}{\partial x_j}[(\mu + \frac{\mu_t}{\sigma_k})\frac{\partial k}{\partial x_j}] + \frac{1}{2}(P_{ii} + G_{ii}) + S_k \tag{9}$$

Where S_k is the source term, as it is clear, the Eq. (9) is the same as Eq. (1). But the difference is in the calculation of k. The k obtained from Eq. (9) is valid wherever in the boundary condition and in any other cases the k would be obtained as Eq. (10).

$$k = \frac{1}{2}\overline{u_i' u_i'} \tag{10}$$

The dissipation tensor would be followed as below:

$$\varepsilon_{ij} = \frac{2}{3}\delta_{ij}\rho\varepsilon \tag{11}$$

And the scalar dissipation rate, ε would be also according to Eq. (12) same as for the standard $k-\varepsilon$ model:

$$\frac{\partial}{\partial t}(\rho\varepsilon) + \frac{\partial}{\partial x_j}(\rho\varepsilon u_j) = \frac{\partial}{\partial x_j}[(\mu + \frac{\mu_t}{\sigma_\varepsilon})\frac{\partial k}{\partial x_j}]C_{\varepsilon 1}\frac{1}{2}[P_{ii} + C_{\varepsilon 3}G_{ii}]\frac{\varepsilon}{k} - \rho C_{\varepsilon 2}\frac{\varepsilon^2}{k}S_\varepsilon \tag{12}$$

Where the S_ε is the source term (if any) and constants are listed in Table 3.

TABLE III VALUE FOR CONSTANTS IN RSM

Coefficient	σ_k	σ_ε	$C_{\varepsilon 1}$	$C_{\varepsilon 2}$
Value	0.82	1	1.44	1.92

The term, $C_{\varepsilon 3}$ is also evaluated as a function of local flow direction like standard $k-\varepsilon$ model as Eq. (13).

$$C_{\varepsilon 3} = \tanh\left|\frac{v}{u}\right| \tag{13}$$

III. NUMERICAL METHOD

A (CFD) finite volume based commercial code (Fluent 6.3), was employed to discrete the momentum, Energy and turbulence transport equations for the case study involved in this paper. The schematic view of the channel is shown in Fig. (1).

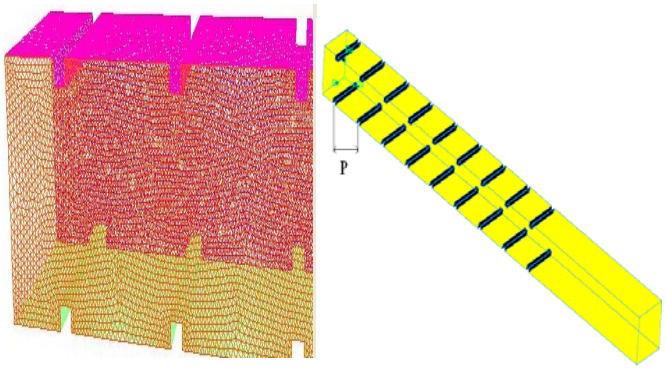

Fig. 1 Schematic view of channel and closer view with tetrahedral/hybrid meshes

The geometry of the case and specification of numerical method used are tabulated in Table 4.

TABLE IV CHANNEL GEOMETRY AND NUMBER OF GRID USED FOR NUMERICAL METHODS

ITEM	$k-\varepsilon$	$k-\omega$	$k-\varepsilon$ Realizable	RSM
Channel length(cm)	195	195	195	195
Channel width(cm)	15	15	15	15
Channel height(cm)	15	15	15	15
Number of ribs(cm)	9	9	9	9
Aspect ratio(e/Dh)	0.1	0.1	0.1	0.1
Pitch to height(p/e)	10	10	10	10
Number of grids(cm)	480000	480000	1600000	2700000

In all four methods the meshes were selected as tetrahedral/hybrid scheme and the y^+ criterion were satisfied in each method. The y^+ was satisfied between 30 to 50 for $k-\varepsilon$ and $k-\omega$ model, between 2 to 10 for $k-\varepsilon$ *realizable* and between 1 to 10 for RSM method, near the wall boundary regions. The boundary conditions for inlet and outlet were velocity inlet and pressure outlet, respectively. In addition the all of the walls temperature was fixed in 1200°K. The Re=20000 in all cases except the graphs involving the centerline velocity and root mean-square velocities (Re=10000).

IV. RESULTS AND DISCUSSIONS

Many efforts and detailed measurements have been done in the field of turbine blade cooling and separation flow around different ribs, but a comparison of time consuming and academic approaches with industrial and practical ones is of interest in this paper.

Because of validation of current results, some plots like the centerline velocities, mean-square velocity at the centerline and Nu number between ribs 2-3 and 5-6 were validated with previous work by Sewall et all [27]. The centerline stream wise velocity of current work with the experiments done with Sewall is shown in Fig. (2)

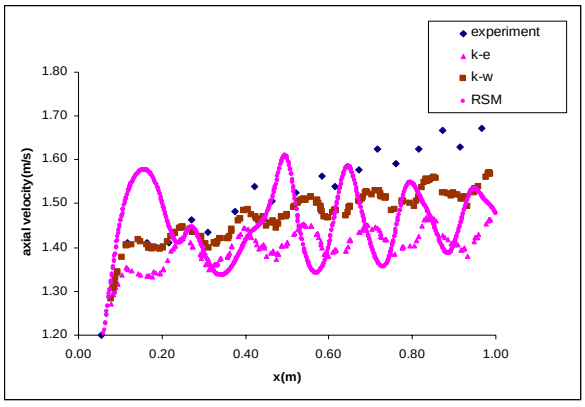

Fig. 2 The centerline stream wise velocity (Re=10000)

As it is shown in Fig. (2), the $k-\varepsilon$ model in comparison with two other methods predicts the lowest values and RSM method has the best results. The main reason that the $k-\omega$ model predicts the velocity better than $k-\varepsilon$, seems to be because of natural characteristics of the model, i.e., the $k-\omega$ model is a low Reynolds model and $k-\varepsilon$ is suitable for high Re number (Re>50000). Indeed, this is not a strong rule and as it will be seen later, the $k-\varepsilon$ model has strong ability in predicting the thermal flux at the wall boundary. Another attractive mater is the behavior of RSM model in predicting the axial velocity; the plot for RSM shows more sever deviation from the mean velocity rather than two other models. The amplitude is high and seems to have difference in this matter with the experimental data but the value of maximum velocity reported by RSM model is somewhere closer to experimental data rather than two other models.

Other comparisons were done in strength of the models employed in the prediction of the heat transfer coefficient between two ribs. Regarding to this goal, a non dimensional Nu number which is defined as Eq. (14),

$$\frac{Nu}{Nu_0} = \left(\frac{q''}{T_s - T_b}.\frac{D_h}{k}\right)/(0.023\,\mathrm{Re}^{.8}\,\mathrm{Pr}^{.4}) \quad (14)$$

was applied to investigate the thermal flux between ribs 2-3. This definition is in accordance with the reported definition by Sewall [27]. In addition, due to high wall temperature and variation of specific heat capacity with temperature, a temperature dependent polynomial was considered as Eq. (15).

$$C_p = 1005.7 - 0.44\,T + 0.001407\,T^2 - 7.99\times10^{-7}\,T^3 + 1.9327\times10^{-10}\,T^4 \quad (15)$$

The non dimensional Nu number is illustrated in Fig. (3).

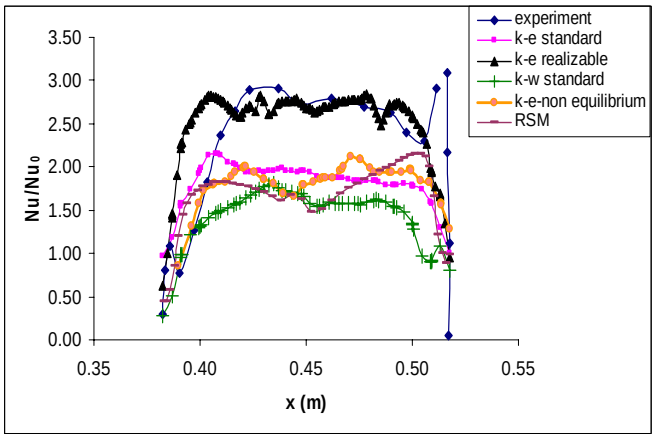

Fig. 3 Non dimensional Nu number between ribs 2 and 3

According to Fig. (3), the predicted values of thermal flux by $k-\varepsilon$ model are better than the $k-\omega$ and RSM model. But the best results are reported by $k-\varepsilon$ *realizable* model. One of the main reasons of three other models seems to be in order of the role of wall function. In fact, the RSM model had the most meshes in compare with three other models but near wall region was treated by wall function. But the $k-\varepsilon$ *realizable* model employs a two layer approach and when there are some computational nodes in the viscose sub layer, takes advantage of them to predict more precise results

on solid boundaries. This manner was repeatedly done between ribs 5 and 6 and results are demonstrated in Fig. (4).

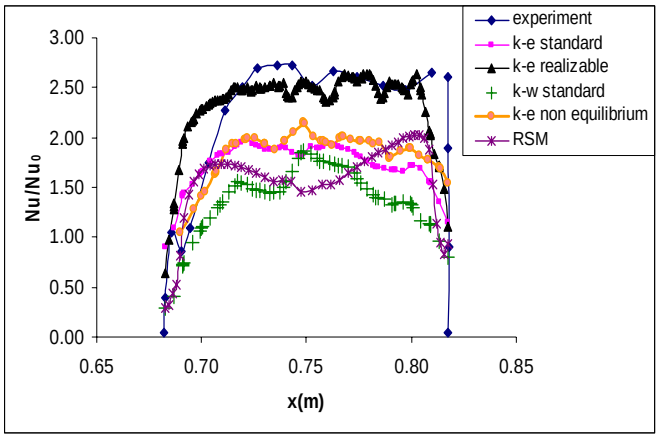

Fig. 4 Non dimensional Nu number between ribs 5 and 6

As shown in Fig. (5), the same manner was observed and $k-\varepsilon$ *realizable* model had the best results.

After validation of numerical results with experimental ones in literature, some attractive characteristics like pressure drop along the channel and the velocity profile and kinetic energy among selected ribs were plotted.

The first graph is dedicated to pressure drop and is illustrated in Fig. (5).

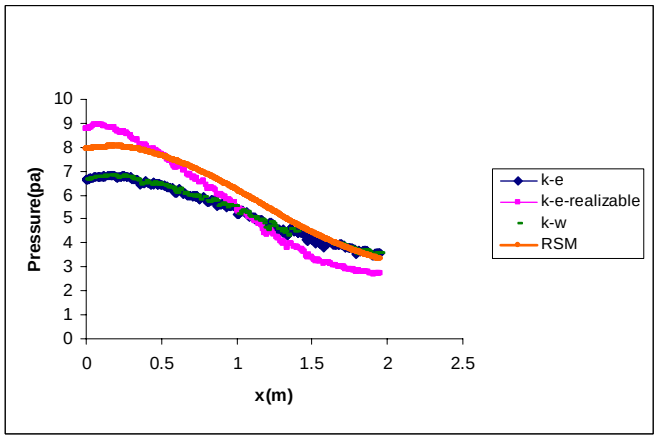

Fig. 5 Pressure drop along the channel

As shown in Fig. (5), the $k-\varepsilon$ and $k-\omega$ model failed to predict the correct pressure drop along the channel centerline and two other models were approximately predicted the same value. One of the reasons of uncertainty of reported values by reported by $k-\varepsilon$ and $k-\omega$ model was related to the steep of the plot. Due to existence of multiple ribs in the channel walls, the slight steep is not reasonable and the two other models manner seems to be in more accordance with reality.

One of the interesting properties of a turbulent flow is the behavior of kinetic energy among the ribs. Therefore the plot of kinetic energy was plotted between ribs 1, 2 and 5, 6 and after the last rib according to Figs. (6-8).

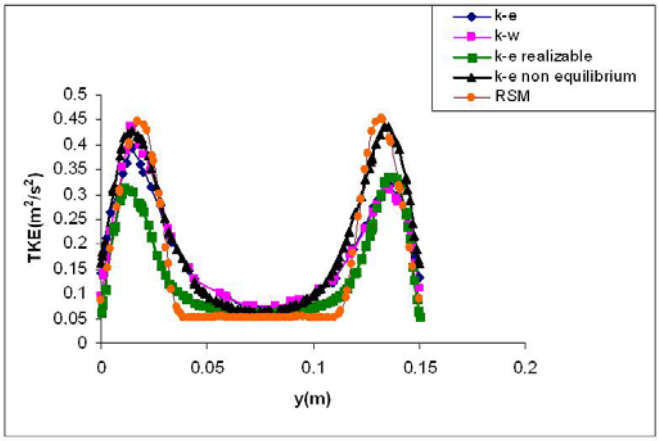

Fig. 6 Plot of kinetic energy between ribs 1 and 2

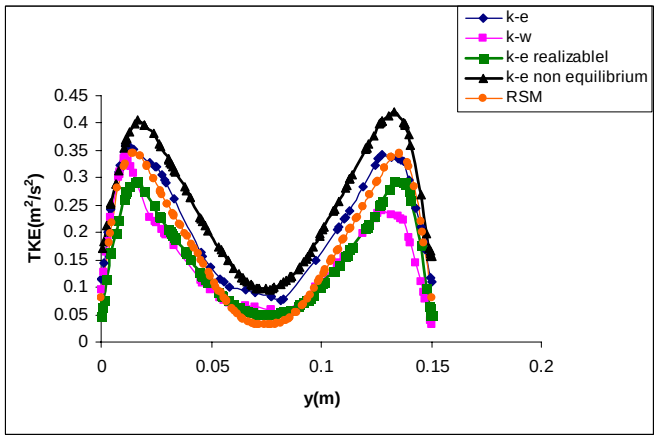

Fig. 7 Plot of kinetic energy between ribs 5 and 6

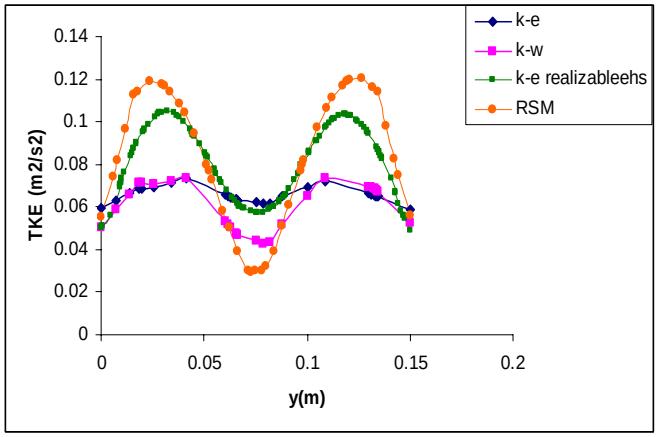

Fig. 8 Plot of kinetic energy after the last rib

As shown in Figs. (6-8), the turbulent kinetic energy increases along the channel but this manner only is valid just before the last rib and after that the kinetic energy decreases dramatically. This shows the effect of ribs in making the severe turbulence among ribs. Another issue is related to the strength of the models in predicting the TKE. As seen, between ribs 1 and 2, the results of RSM and $k-\varepsilon$ non

equilibrium are so similar to each other and between ribs 5 and 6 the kinetic energy value reported by RSM, $k-\varepsilon$ and $k-\varepsilon$ non equilibrium was coincident. This behavior completely changes after the last rib. The results of RSM model have the similarity with the results of $k-\varepsilon$ *realizable* near the channel wall and have similarity with $k-\omega$ model near the centerline. Generally speaking, the best results seem to be reported by RSM model and weakest ones by $k-\omega$ model.

Due to better comprehension of behavior of turbulence, the velocity profiles are plotted among the above mentioned ribs as for kinetic energy.

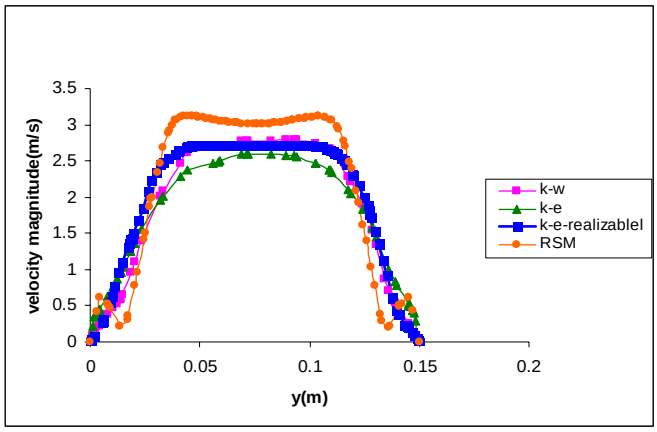

Fig. 9 Velocity profile between ribs 1 and 2

As shown in Fig. (9), the turbulent flow is not yet formed and upper surface of plot is flat but by moving forward along the channel, the profile becomes completely parabolic as shown in Fig. (10). In addition the RSM model has reported the highest value rather than three other models.

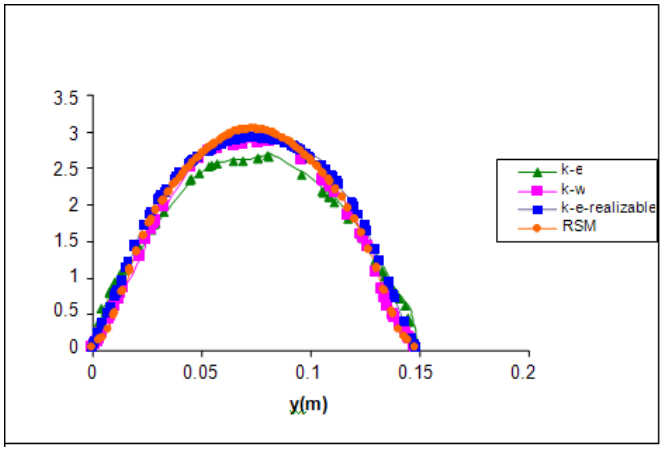

Fig. 10 Velocity profile between ribs 5 and 6

According to Figs. (9 & 10), all of the models has nearly predicted the same value and behavior, but the $k-\varepsilon$ value predicted by model are less than the others. The next graph was plotted after the ribs as shown in Fig. (11).

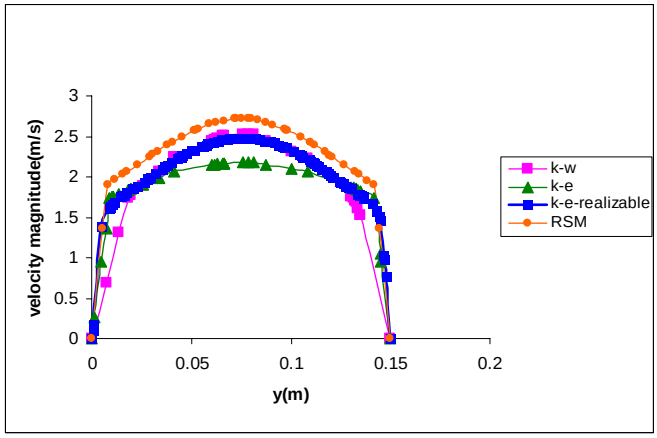

Fig. 11 Velocity profile after the last rib

As seen in Fig. (11), the velocity profile tends to become flat and this means the fully developed flow after the ribs. The fascinating matter is in the behavior of $k-\varepsilon$ *realizable* in which the velocity values near the channel wall are completely in accordance with the values of $k-\varepsilon$ and in the core region are completely matched with $k-\omega$ model. It seems that the best results are reported by $k-\varepsilon$ *realizable* model and results of RSM model are not so satisfactory.

It should be noticed that the velocity profiles are plotted in the line which has connected the left wall to the right one. If the graphs were suppose to be plotted in the line vertical to this line, no special behavior was found and a flat profiles were obtained for all of the situations and actually the formation of fully turbulent flow was not observable.

V. CONCLUSIONS

A (CFD) Finite Volume method was applied to investigate the effect of turbulence models in predicting the fluid flow and heat transfer in a three dimensional square-ribbed channel with the constant wall temperature. The results show that there is not a specific model to predict all of the turbulence properties accurately. The $k-\varepsilon$ *realizable* model was considered as the best model for predicting the heat transfer coefficient and after that the $k-\varepsilon$ model was the best, in addition, the $k-\omega$ and $k-\varepsilon$ *realizable* model were powerful in prediction of velocity profile, the RSM model was the best in predicting the kinetic energy

ACKNOWLEDGMENT

With especial thanks to Mr. Farajpour because of his guides for RSM method section.

REFERENCES

[1] Han, J.C., Park, J.S., 1988. "Developing heat transfer in rectangular channels with rib turbulators". *International Journal of Heat and Mass Transfer* 31 (1), 183–195.

[2] Liou, T.-M., Hwang, J.-J., 1992a. "Developing heat transfer and friction in a ribbed rectangular duct with flow separation at inlet". *ASME Journal of Heat Transfer* 114, 565–573.

[3] Wagner, J.H., Johnson, B.V., Graziani, R.A., Yeh, F.C., 1992. "Heat transfer in rotating serpentine passages with trips normal to the flow". *ASME Journal of Turbomachinery* 114, 847–857.

[4] Wang, L.-B., Tao, W.-Q., Wang, Q.-W., Wong, T.T., 2001. "Experimental study of developing turbulent flow and heat transfer in ribbed convergent/divergent square ducts". *International Journal of Heat and Fluid Flow* 22, 603–613.

[5] T.-H. Shih, W.W. Liou, A. Shabbir, Z. Yang, and J. ZhuA. 1995. "New k-e Eddy Viscosity Model for High Reynolds Number Turbulent Flows-Model Development and Validation". *Computers and Fluids* 24(3): 227-238.

[6] Chang, S.W., Morris, W.D., 2003. "Heat transfer in a radially rotating square duct fitted with in-line transverse ribs". *International Journal of Thermal Sciences* 42, 267–282.

[7] Han, J.C., 1984. "Heat transfer and friction in channels with two opposite rib-roughened walls". *ASME Journal of Heat Transfer* 106, 774–781.

[8] Liou, T.-M., Hwang, J.-J., 1992b. "Turbulent Heat Transfer Augmentation and Friction in Periodic Fully Developed Channel Flows". *ASME Journal of Heat Transfer* 114, 56–64.

[9] Baughn, J.W., Yan, X., 1992. Local heat transfer measurements in square ducts with transverse ribs. *ASME HTD, Enhanced Heat Transfer* 202,1–7.

[10] Fann, S., Yang, W.-J., Zhang, N., 1994. "Local heat transfer in a rotating serpentine passage with rib-roughened surfaces". *International Journal of Heat and Mass Transfer* 37 (2), 217–228.

[11] Park, C.W., Lau, S.C., Kukreja, R.T., 1998." Heat/mass transfer in a rotating two-pass channel with transverse ribs". *Journal of Thermophysics and Heat Transfer* 12 (1), 80–86.

[12] Mochizuki, S., Murata, A., Shibata, R., Yang, W.-J., 1999. "Detailed measurements of local heat transfer coefficients in turbulent flow through smooth and rib-roughened serpentine passages with a 180_ sharp bend". *International Journal of Heat and Mass Transfer* 42, 1925–1934.

[13] Ekkad, S.V., Pamula, G., Shantiniketanam, M., 2000. "Detailed heat transfer measurements inside straight and tapered two-pass channels with rib turbulators". *Experimental Thermal and Fluid Science* 22, 155–163.

[14] Chen, Y., Nikitopoulos, D.E., Hibbs, R., Acharya, S., Myrum, T.A.,2000. "Detailed mass transfer distribution in a ribbed coolant passage with a 180_ bend". *International Journal of Heat and Mass Transfer* 43,1479–1492.

[15] Islam, M.S., Haga, K., Kaminaga, M., Hino, R., Monde, M., 2002. "Experimental analysis of turbulent flow structure in a fully developed rib-roughened rectangular channel with PIV". *Experiments in Fluids* 33, 296–306.

[16] Rau, G., C¸ akan, M., Moeller, D., Arts, T., 1998. "The effect of periodic ribs on the local aerodynamic and heat transfer performance of a straight cooling channel". *ASME Journal of Turbomachinery* 120, 368–375.

[17] Sato, H., Hishida, K., Maeda, M., 1989. "Turbulent flow characteristics in a rectangular channel with repeated rib roughness". *ASME HTD, Heat Transfer in Convective Flows* 107, 191–196.

[18] Liou, T.-M., Wu, Y.-Y., Chang, Y., 1993a." LDV measurements of periodic fully developed main and secondary flows in a channel with rib disturbed walls". *ASME Journal of Fluids Engineering* 115, 109–114.

[19] Graham, A., Sewall, E., Thole, K.A., 2004. "Flow field measurements in a ribbed channel relevant to internal turbine blade cooling". In: *Proceedings of the ASME Turbo Expo 2004, Vienna, Austria*, ASME Paper No. GT2004-53361.

[20] Hirota, M., Yokosawa, H., Fujita, H., 1992. "Turbulence kinetic energy in turbulent flows through square ducts with rib-roughened walls". *International Journal of Heat and Fluid Flow* 13 (1), 22–29.

[21] Durst, F., Founti, M., Obi, S., 1988. "Experimental and computational investigation of the two-dimensional channel flow over two fences in tandem". *ASME Journal of Fluids Engineering* 110, 48– 54.

[22] Liou, T.-M., Chang, Y., Hwang, D.-W., 1990. "Experimental and computational study of turbulent flows in a channel with two pairs of turbulence promoters in tandem". *ASME Journal of Fluids Engineering* 112, 302–310.

[23] Acharya, S., Dutta, S., Myrum, T.A., Baker, R.S., 1993." Periodically developed flow and heat transfer in a ribbed duct". *International Journal of Heat and Mass Transfer* 36 (8), 2069–2082.

[24] Prakash, C., Zerkle, R., 1995. "Prediction of turbulent flow and heat transfer in a ribbed rectangular duct with and without rotation". *ASME Journal of Turbomachinery* 117, 255–264.

[25] Zhao, C.Y., Tao, W.Q., 1997. "A three dimensional investigation of turbulent flow and heat transfer around sharp 180-deg turns in two pass rib-roughened channels". *International Communications in Heat and Mass Transfer* 24 (4), 587–596.

[26] Ooi, A., Iaccarino, G., Durbin, P.A., Behnia, M., 2002. "Reynolds averaged simulation of flow and heat transfer in ribbed ducts". *International Journal of Heat and Fluid Flow* 23, 750–757.

[27] Evan A. Sewall, Danesh K. Tafti, Andrew B. Graham, Karen A. Thole. "Experimental validation of large eddy simulations of flow and heat transfer in a stationary ribbed duct". *International Journal of Heat and Fluid Flow* 27 (2006) 243–258.

[28] Saha, A.K., Acharya, S., 2003. "Flow and heat transfer in an internally ribbed duct with rotation: an assessment of LES and URANS". In: *Proceedings of the ASME Turbo Expo 2003, Atlanta, Georgia, USA*, ASME Paper No. GT2003-38619.

[29] Tafti, D.K., 2005. "Evaluating the role of subgrid stress modeling in a ribbed duct for the internal cooling of turbine blades". *International Journal of Heat and Fluid Flow* 26, 92–104.

[30] Abdel-Wahab, S., Tafti, D.K., 2004b. "Large eddy simulation of flow and heat transfer in a staggered 45_ ribbed duct". In: *Proceedings of the ASME Turbo Expo 2004, Vienna, Austria*, ASME Paper No. GT2004-53800.

[31] Bonhoff, B., Tomm, U., Johnson, B.V., Jennions, I., 1997. "Heat transfer predictions for rotating u-shaped coolant channels with skewed ribs and with smooth walls". In: *Proceedings of the International Gas Turbine & Aeroengine Congress & Exhibition, Orlando, Florida, USA*, Paper No. 97-GT-162.

[32] Lin, Y.-L., Shih, T.I.-P., Stephens, M.A., Chyu, M.K., 2001. "A numerical study of flow and heat transfer in a smooth and ribbed U-duct with and without rotation". *ASME Journal of Heat Transfer* 123, 219–232.

[33] Jang, Y.-J., Chen, H.-C., Han, J.-C., 2001. "Flow and heat transfer in a rotating square channel with 45 deg angled ribs by Reynolds stress turbulence model". *ASME Journal of Turbomachinery* 123, 124–132.

[34] Al-Qahtani, M., Jang, Y.-J., Chen, H.-C., Han, J.-C., 2002a." Prediction of flow and heat transfer in rotating two-pass rectangular channels with 45-deg rib turbulators". *ASME Journal of Turbomachinery* 124, 242–250.

[35] Al-Qahtani, M., Chen, H.-C., Han, J.-C., 2002b." A numerical study of flow and heat transfer in rotating rectangular channels (AR = 4) with 45_ rib turbulators by Reynolds stress turbulence model". In: *Proceedings of the ASME Turbo Expo 2002, Amsterdam, The Netherlands,*ASME Paper No. GT- 2002-30216.

[36] Murata, A., Mochizuki, S., 2001. "Comparison between laminar and turbulent heat transfer in a stationary square duct with transverse or angled rib turbulators". *International Journal of Heat and Mass Transfer* 44, 1127–1141.